# Silicon and carbon vacancies in neutron-irradiated SiC: A high-field electron paramagnetic resonance study

S. B. Orlinski and J. Schmidt
*Huygens Laboratory, Department of Physics, Leiden University, P.O. Box 9504, 2300 RA Leiden, The Netherlands*

E. N. Mokhov and P. G. Baranov
*A.F. Ioffe Physico-Technical Institute, Polytekhnicheskaya 26, 194021, St. Petersburg, Russia*

(Received 17 January 2002; revised manuscript received 12 November 2002; published 27 March 2003)

Electron-paramagnetic-resonance (EPR) and electron-spin-echo (ESE) studies have been performed that show that isolated $V_{Si}^{-}$, $V_{Si}^{0}$, and $V_C$ vacancies are the dominant intrinsic paramagnetic defects in SiC treated by room-temperature neutron irradiation with doses up to $10^{19}$ cm$^{-2}$. This conclusion is supported by the observation of high concentrations of all these defects in 4H- and 6H-SiC that are almost proportional to the irradiation dose. The 95-GHz EPR spectra at 1.2 K prove that the ground state of $V_{Si}^{0}$ corresponds to $S=1$ and that the zero-field splitting parameter $D$ is positive. A possible energy-level scheme and optical pumping process which induces the spin polarization of the ground triplet state of the $V_{Si}^{0}$ vacancy in SiC is presented. In the EPR spectra of $V_{Si}^{-}$ in 4H-SiC an anisotropic splitting of the EPR lines is observed. This splitting is assumed to arise from small differences in the $g$ tensor of the quasicubic ($k$) and hexagonal ($h$) sites. Anisotropic EPR spectra with $S=\frac{1}{2}$ that are related to the carbon vacancy have also been observed in the $n$-irradiated SiC crystals. The hyperfine (hf) interaction with the first shell of Si atoms is almost identical to that observed in electron-irradiated SiC crystals. The observed additional 6.8-G hf splitting with 12 carbon atoms in the second shell is considered as a confirmation for the isolated carbon vacancy model.

DOI: 10.1103/PhysRevB.67.125207 PACS number(s): 71.55.−i, 61.72.Ww

## I. INTRODUCTION

Silicon carbide (SiC) is a promising wide band-gap semiconductor for applications in high-frequency, high-temperature, high-power, and radiation-resistant electronic devices. The main doping method is by ion implantation because very high temperatures are needed for doping of SiC by diffusion. The ionic implantation produces unwanted damages in the SiC lattice that are difficult to repair, because some defects remain even after a 2000 °C anneal. Therefore the investigation of the radiation defects in SiC is of great importance also in view of the potential application of SiC-based devices for operation in radiation surroundings.

The primary defects that can be produced in binary compound SiC are vacancies, interstitials, and antisites. In contrast to silicon[1] the primary defects in SiC seem to be stable at, and even far above, room temperature. These primary defects are present at the various sites in the different polytypes that arise from differences in the stacking sequence of the Si and C layers. The hexagonal 4H and 6H polytypes are the most common and most appropriate for applications. In 4H-SiC two nonequivalent crystallographic positions exist, one hexagonal and one quasicubic site, called $h$ and $k$, respectively. In 6H-SiC three nonequivalent positions are formed, one hexagonal and two quasicubic ones, called $h$, $k_1$, and $k_2$.

Two important experimental tools for the identification and study of the defects in SiC are electron-paramagnetic resonance (EPR) and optically detected magnetic resonance (ODMR).[2–12] EPR investigations have revealed the presence of only two charge states of the Si vacancy.[5,6,8–11] Very sophisticated EPR investigations also show the existence of Si-related Frenkel pairs in SiC.[12] The identification of carbon vacancies is presently still under debate.

The dominant EPR spectrum with an isotropic $g$ factor $g=2.0032$, that can be observed in electron-, neutron-, or proton-irradiated SiC crystals up to room temperature, was attributed to the negatively charged isolated silicon vacancy $V_{Si}^{-}$ with $S=\frac{3}{2}$.[5,6,8,11] The anisotropic hyperfine (hf) structure caused by the interaction with the four nearest-neighbor carbon atoms (the first shell) and the almost isotropic hyperfine structure caused by the interaction with 12 next-nearest-neighbor silicon atoms (the second shell) were observed in the EPR spectra. No site dependence was detected for $V_{Si}^{-}$. The experimental results are supported by theoretical calculations[5,8] that predict that the ground state of $V_{Si}^{-}$ corresponds to a high-spin configuration with $S=\frac{3}{2}$.

The second type of EPR spectra, observed by several groups,[4,7,9–11] is a triplet center ($S=1$) with an isotropic $g$ factor $g=2.0032$ and a site-dependent zero-field splitting parameter $D$. In Refs. 7, 9, and 10 these spectra were detected by ODMR by monitoring the zero-phonon lines (ZPL's) at 1.438 (labeled $V1$) and 1.352 eV ($V2$) in 4H-SiC and 1.433 ($V1$), 1.398 ($V2$), and 1.368 eV ($V3$) in 6H-SiC. The number of ZPL's corresponds to the number of inequivalent lattice sites in these polytypes. The authors of Refs. 9 and 10 were the first to attribute these EPR spectra to the neutral isolated Si vacancy ($V_{Si}^{0}$). This assignment was based on the observed characteristic hf structure with the 12 Si atoms of the second shell that resembled the hf structure for the negatively charged isolated silicon vacancy $V_{Si}^{-}$. Further support for this assignment was supplied later by the observation of the hf interaction with the four nearest carbon atoms.[13] For 4H-SiC the zero-field splitting parameter $D$ was found to be $22\times10^{-4}$ cm$^{-1}$ and $13\times10^{-4}$ cm$^{-1}$ for the $h$ (ZPL $V2$) and $k$ ($V1$) sites, respectively. For 6H-SiC $D=42.8\times10^{-4}$ cm$^{-1}$ and $9\times10^{-4}$ cm$^{-1}$ for the $h$ ($V2$) and $k$ sites

 

($V1$, $V2$ lines; the two sites $k_1$ and $k_2$ were not resolved by EPR). The site identification was made by assuming that a defect at a hexagonal site experiences a stronger axial crystal field than a defect on a quasicubic site and that consequently the zero-field splitting for the hexagonal site is larger than that for the quasicubic site.

In the case of $V_{Si}^0$ there exist two opposite points of view concerning the spin multiplicity of the ground state. Based on experimental studies either a singlet[4,9,10] or a triplet[11] ground state was suggested. This problem has been the subject of several theoretical studies and a ground state with $S=0$,[14,15] as well as $S=1$,[16,17] has been predicted.

It is clear that more experimental information is needed to solve the problems concerning the silicon vacancies in SiC. First, it is of importance to confirm which spin multiplicity corresponds to the ground state of the neutral isolated silicon vacancy $V_{Si}^0$. Moreover, it would be attractive to determine the sign of the zero-field splitting parameter $D$, i.e., the ordering of the spin sublevels, and the details of the optical pumping process which induces the spin polarization of the triplet state. Second, with regard to $V_{Si}^-$, it is interesting to check whether there is a site dependence of the $g$ tensor and whether a zero-field splitting can be observed for this center. Preliminary results of an EPR study of the isolated silicon vacancies in *n*-irradiated 4H-SiC that solved part of these problems were presented in Ref. 18.

The studies of the carbon vacancies in SiC published so far[5,18–20] have led to contradicting conclusions. The spectra reported by Itoh *et al.*[5] were suggested to belong to a hydrogen-related defect[19] whereas the spectra observed by the authors of Refs. 18–20 seem to belong to the positively charged isolated carbon vacancy $V_C^+$. Here we present more extensive results than in our previous publication[20] of an EPR study on the carbon vacancy in *n*-irradiated SiC. The observed EPR spectra exhibit parameters characteristic for the $V_C$ center. Importantly the hf structure of the 12 carbon atoms of the second shell, that can be considered as a confirmation of $V_C$, has been observed. In addition, the high concentration of $V_C$ centers that observed in *n*-irradiated SiC excludes its extrinsic character.

## II. EXPERIMENT

The samples used in this study were Lely-grown *n*-type 4H-SiC and 6H-SiC with concentrations of uncompensated nitrogen in the range $10^{16}$–$10^{17}$ cm$^{-3}$. These samples were irradiated at room temperature (RT) with neutrons with doses ranging from $10^{15}$ to $10^{20}$ cm$^{-2}$. No annealing treatment was applied.

The experiments were performed at 1.2–300 K on a home-built, pulsed EPR spectrometer operating at a microwave frequency of 94.9 GHz.[21] The main advantages of this spectrometer are the high resolution in both the EPR and the electron-nuclear double resonance (ENDOR) measurements and, owing to the split-coil configuration of the superconducting magnet, the possibility to perform a complete orientational study. The pulsed electron-spin-echo (ESE)-detected EPR spectra were measured using a two-pulse echo experiment, in which the electron-spin-echo intensity is monitored as a function of the magnetic field. EPR measurements were also performed on Bruker-680 X-band (9.4 GHz) and W-band (94.9 GHz) continuous wave (cw) EPR spectrometers.

The samples, in the shape of platelets, had dimension of about $3\times4\times0.4$ mm$^3$ for X-band and sizes of $0.3\times0.4\times0.5$ mm$^3$ for W-band EPR experiments. The samples were oriented for rotation in the {11-20} plane. All calculations were made using the computer package VISUAL EPR written by Grachev, which performs numerical diagonalization of the spin Hamiltonian matrix.[22]

## III. RESULTS AND DISCUSSION

Several EPR and ESE spectra were detected in neutron-irradiated 4H- and 6H-SiC crystals. The dominant spectra at 300 K that could be observed for doses ranging from $10^{15}$ to $10^{19}$ cm$^{-2}$ are attributed to $V_{Si}^-$ and $V_{Si}^0$ vacancies. At low temperature the anisotropic EPR spectra of carbon vacancies were detected together with the signals of $V_{Si}^-$ and $V_{Si}^0$.

Figure 1(a) shows cw W-band EPR spectra observed at room temperature in 6H-SiC crystals irradiated by fast neutrons with a dose of $5\times10^{15}$ cm$^{-2}$ (1) and with a dose of $1\times10^{19}$ cm$^{-2}$ (2a, 2b, and 2c). Spectrum 1 was recorded for the magnetic field parallel to the $c$ axis ($B\|c$). Spectra 2a, 2b, and 2c were recorded for angles between the magnetic field and the $c$ axis of 5°, 55°, and 90° ($B\perp c$), respectively.

There are two dominant types of EPR spectra observed in the two types of crystals in Fig. 1(a). The central signal, marked by the oblique solid arrow, is accompanied by a set of hyperfine lines with a splitting of 0.29 mT and an intensity ratio to the central line of about 0.3. These two hf lines correspond to the interaction with 12 equivalent Si atoms of the second shell. This spectrum is attributed to the $V_{Si}^-$ vacancy with $S=\frac{3}{2}$ and $D=0$.[8] The second EPR spectrum indicated by the double arrows is attributed to the $V_{Si}^0$ vacancy ($S=1$) in the hexagonal ($h$) and quasicubic ($k_1$,$k_2$) sites. The horizontal bars of the same level mark the lines that belong to the same center. For 6H-SiC there are two sets of doublets with splittings for $B\|c$ of about 9.0 and 1.9 mT. The intensity of the inner doublet ($k_1$, $k_2$ sites) is two times larger than that of the outer doublet ($h$ site). In addition there are unidentified lines with $S=\frac{1}{2}$ and with an anisotropic $g$ tensor that are indicated by solid vertical arrows and by brackets. These lines will be discussed later.

Figure 1(b) shows cw W-band EPR spectra observed at room temperature in 4H-SiC crystals irradiated by fast neutrons with a dose of $1\times10^{18}$ cm$^{-2}$. The spectra were recorded with the magnetic field parallel and perpendicular to the $c$ axis. Like in Fig. 1(a) the oblique solid arrow indicates the position of the central line of the $V_{Si}^-$ vacancy ($S=\frac{3}{2}$) and the double arrows indicate the positions of the lines of the $V_{Si}^0$ vacancy ($S=1$) in different sites ($h$ and $k$). For 4H-SiC there are two sets of doublets with equal intensity and splittings of about 4.7 and 2.8 mT, respectively. The high-gain spectrum ($\times20$) shows the hf structure for the triplet state $V_{Si}^0$ vacancy in 4H-SiC. One can see that the spectra consist of a central line and two satellites with a splitting of

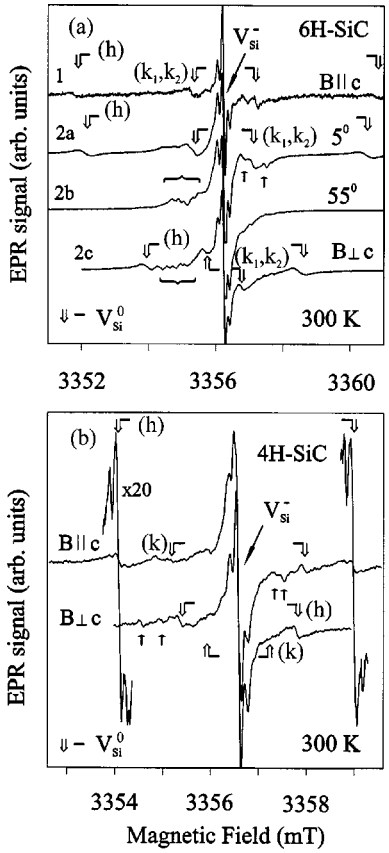


FIG. 1. (a) cw W-band (94.0 GHz) EPR spectra observed at 300 K in 6H-SiC crystals irradiated by fast neutrons with doses of $5\times10^{15}$ cm$^{-2}$ (spectrum 1) and of $1\times10^{19}$ cm$^{-2}$ (spectra 2a–2c). Spectrum 1 was recorded with the magnetic field parallel to the $c$ axis ($B\|c$). Spectra 2a, 2b, and 2c were recorded with angles between the magnetic field and the $c$ axis of 5°, 55°, and 90° ($B\perp c$), respectively. The double vertical arrows indicate the positions of the lines for the $V_{Si}^0$ vacancy ($S=1$) in the hexagonal ($h$) and quasicubic ($k_1$,$k_2$) sites. The horizontal bars connected to the double arrows mark the lines that belong to the same center. The oblique solid arrow indicates the position of the central line of the $V_{Si}^-$ vacancy ($S=\frac{3}{2}, D\cong 0$). Some of unidentified lines with $S=\frac{1}{2}$ and an anisotropic $g$ tensor are indicates by solid vertical arrows and by brackets. (b) cw W-band (94.0 GHz) EPR spectra observed at 300 K in 4H-SiC crystals irradiated by fast neutrons with a dose of $1\times10^{18}$ cm$^{-2}$. The spectra were recorded for the orientations $B\|c$ and $B\perp c$. The double arrows indicate the positions of the lines for the $V_{Si}^0$ vacancy in hexagonal ($h$) and quasicubic ($k$) sites. The high-gain spectrum (×20) shows the hf structure with 12 Si of the second shell for the triplet state $V_{Si}^0$ vacancy in 4H-SiC. The oblique solid arrow indicates the position of the central line of the $V_{Si}^-$ vacancy. Some of unidentified lines of centers with $S=\frac{1}{2}$ and an anisotropic $g$ tensor are indicated by solid vertical arrows.

about 0.3 mT and an intensity ratio to the central line of about 0.3. Such satellites were observed for the $V_{Si}^-$ vacancy [Figs. 1(a) and (b)] and were related to the hf interaction with 12 Si atoms. Thus the typical aspect of the EPR spectra of the silicon vacancy is the isotropic hf structure from 12 silicon atoms of the second shell with a splitting of about 0.3 mT. In the irradiated (neutron, electron, proton) SiC samples one can detect more then 30 triplet centers with different $D$ parameters ranging from almost zero to about 500 G.[2–4] Thus the $D$ parameter cannot be directly linked to the structure of the vacancy. What is more, there is a peculiarity in the value of the $D$ parameters in 4H- and 6H-SiC. The $D$ parameter for the $h$ site in 6H-SiC is almost two times larger than that of 4H-SiC in spite of the fact that the axial crystal field in 4H-SiC is larger. Some of the unidentified lines with $S=\frac{1}{2}$ and an anisotropic $g$ tensor are indicated by solid arrows.

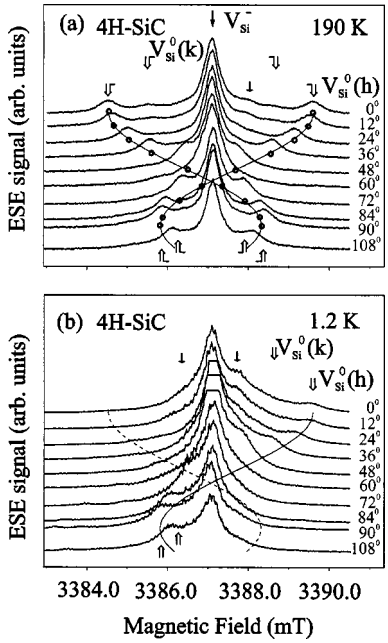


FIG. 2. Angular dependences of ESE spectra observed at 94.9 GHz in $n$-irradiated 4H-SiC (dose of $10^{18}$ cm$^{-2}$) at 190 K (a) and 1.2 K (b). The experimental spectra are shown with steps of 12°. The angle $\theta=0°$ corresponds to the magnetic field parallel to the $c$ axis. The theoretical angular dependences are shown only for the $h$ site. The open circles on the curve [shown only in (a)] correspond to the magnetic-field values of the peaks of the resonances on the baseline of each spectrum. Solid lines correspond to the positions of the experimental EPR lines, the dashed line shows the positions of the EPR lines that are not observable due to the low temperature. The vertical double arrows indicate the positions of the lines for the $V_{Si}^0$ vacancy in the $h$ and $k$ sites for $B\|c$ (top of the figure) and for $B\perp c$ (bottom). Some of unidentified lines of centers with $S=\frac{1}{2}$ and an anisotropic $g$ tensor are indicated by solid vertical arrows.

It is clear that in SiC crystals irradiated at room temperature with neutrons with doses ranging from $10^{15}$ to $10^{19}$ cm$^{-2}$ the $V_{Si}^-$ and $V_{Si}^0$ vacancies are present at high concentrations. We believe that the triplet EPR signals in Figs. 1(a) and (b) belong to the same centers as those detected in the ODMR measurements (the same $D$ and the second-shell Si hf structure parameters) and that were attributed to the $V_{Si}^0$ vacancy. Our first aim is to decide whether the observed triplet spectra belong to the ground state or to an excited state of $V_{Si}^0$. To this end EPR experiments were performed at very low temperatures and in complete darkness to exclude the possibility of a thermal or optically excited triplet state. Figure 2 shows the angular dependences of the ESE-detected EPR spectra observed at W band (94.9 GHz) in $n$-irradiated 4H-SiC ($10^{18}$ cm$^{-2}$) at 190 K (a) and 1.2 K

(b). The experimental spectra are shown for steps of 12°. The angle $\theta = 0°$ corresponds to the magnetic field parallel to the *c* axis. The theoretical dependences are shown only for the *h* position. The open circles on the curve [shown only in Fig. 2(a)] correspond to the magnetic-field values of the peaks of the resonances on the baseline of each spectrum. The solid lines correspond to the positions of the experimental EPR lines, and the dashed line indicates the position of the EPR lines that are not observable due to the low temperature. The vertical double arrows indicate the positions of the lines for the $V_{Si}^0$ vacancy in the *h* and *k* sites for $B \| c$ (top of the figure) and for $B \perp c$ (bottom). Some of the unidentified lines with $S = \frac{1}{2}$ and an anisotropic *g* tensor are indicated by solid arrows. Similar dependences of the ESE-detected EPR spectra were observed for the $V_{Si}^0$ vacancy in 6H-SiC. At 1.2 K only one line was also observed for the triplet state of each site in 6H-SiC (*h*, $k_1$, and $k_2$).

The triplet EPR signals are very strong at low temperature. Thus we conclude that we are dealing with a triplet ground state. It should be noted that in the EPR spectra at 1.2 K the intensities of the fine-structure components differ strongly due to the extreme difference in the populations of the triplet sublevels at this low temperature and the large Zeeman splitting. This result allows us to decide that the *D* parameter of the $V_{Si}^0$ vacancy is positive in 4H-SiC and 6H-SiC for all the sites. The main conclusion is that the ground state of the $V_{Si}^0$ vacancy in SiC corresponds to a triplet state.

In the same *n*-irradiated SiC crystals ESE-detected EPR lines of other triplet centers were observed. The spectra were observed at 1.2 K without illumination and can be described with an axial spin Hamiltonian for $S = 1$ with the principal axis along the *c* axis and with parameters $D \cong 400 \times 10^{-4}$ cm$^{-1}$ and $g = 2.003$. In addition less intense ESE spectra of triplet centers also with *D* parameters of about $400 \times 10^{-4}$ cm$^{-1}$ but with the principal axes not oriented along the *c* axis were observed at 1.2 K without illumination. This spectrum seems to belong to the same type of centers observed by Vainer and Il'in[4] and labeled by them as *P*6. These authors observed this spectrum only under illumination of the sample and they suggested[4] that it belongs to an excited triplet state similar to the case of the $V_{Si}^0$ vacancy. Since we observe the spectrum with similar parameters at the very low temperature of 1.2 K without illumination we conclude that this center has a triplet ground state with a positive *D* parameter. Vainer and Il'in[4] attributed these spectra to the triplet excited state of the Si-C divacancy, but recently these spectra were assigned to the excited state to the $C_{Si}$-$V_C$ pair by Lingner *et al.*[23]

Next, we consider the negatively charged $V_{Si}^-$ vacancy. Here we used 95-GHz EPR to find a site dependence in the EPR spectra. Figure 3(a) shows cw 95-GHz EPR spectra of the $V_{Si}^-$ vacancy observed at 300 K in *n*-irradiated 4H-SiC ($10^{18}$ cm$^{-2}$) for several orientations of the magnetic field with respect to the *c* axis, including the orientations parallel ($\theta = 0°$) and perpendicular ($\theta = 90°$) to the *c* axis. The central line and two hf satellites are shown for the *h* and *k* sites. The intensity ratio of the central line to the satellites corresponds to the interaction with 12 silicon nuclei of the second shell. A very small splitting is observed of the central line that is most pronounced for the magnetic field parallel to the *c* axis and that is caused by a small difference in the $g_\parallel$ values of the *h* and *k* sites. The spectra are slightly anisotropic with a *g*-tensor anisotropy of about $10^{-5}$. This anisotropy is too small to be detected at X band, that is why as yet no site dependence of the EPR spectra of the $V_{Si}^-$ vacancy was observed.

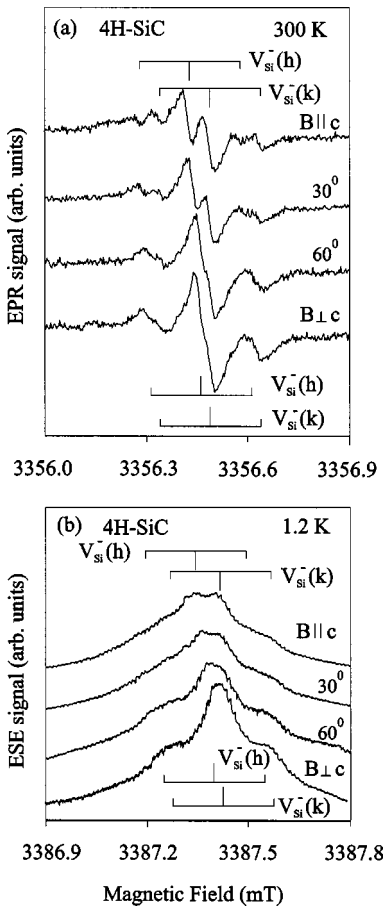


FIG. 3. (a) cw W-band (94.9 GHz) EPR spectra of the $V_{Si}^-$ vacancy observed at 300 K in *n*-irradiated 4H-SiC (dose of $10^{18}$ cm$^{-2}$) for several orientations of the magnetic field with respect to the *c* axis including the orientations parallel ($\theta = 0°$) and perpendicular ($\theta = 90°$) to the *c* axis. The central line and two hf satellites are shown for the *h* and *k* sites. The intensity ratio of the central line to that of the satellites corresponds to the interaction with 12 silicon nuclei of the second shell. (b) W-band (94.9 GHz) ESE spectra of the $V_{Si}^-$ vacancy observed at 1.2 K in *n*-irradiated 4H-SiC (dose of $10^{18}$ cm$^{-2}$) for several orientations of the magnetic field with respect to the *c* axis including the orientations parallel ($\theta = 0°$) and perpendicular ($\theta = 90°$) to the *c* axis.

The splitting shown in Fig. 3(a) is assumed to arise from small differences in the *g* tensor of the quasicubic and hexagonal sites. The *g* factor for the *k* site $g(k)$ is found to be isotropic with $g(k) = 2.0032$ and the *g* factor of the *h* site is found to be slightly anisotropic with $g_\parallel(h) - g(k) = 0.000\,04$ and $g_\perp(h) - g(k) = 0.000\,02$. These differences in *g* factors can be measured with a much higher precision than the absolute *g* values due to the lack of a precise and reliable *g*

marker for high-frequency EPR. The site identification has been made assuming that a defect at the hexagonal site experiences a stronger axial crystal field than a defect in the quasicubic site. It should be noted that to detect the sign and value of these small changes in the position of the line in high magnetic fields we used as a marker the EPR signal of the $V_{Si}^-$ vacancy in *n*-irradiated cubic 3C-SiC. In this crystal the *g* tensor is assumed to be isotropic. The 3C-SiC sample was placed in the cavity simultaneously with the hexagonal 4H-SiC sample. It was found that the *g* tensors of the $V_{Si}^-$ vacancy in 3C-SiC and of the $V_{Si}^-$ vacancy in the cubic site in 4H-SiC practically coincide.

The EPR measurements at 95 GHz allows us to check the assignment of the spin multiplicity of $V_{Si}^-$ and $V_{Si}^0$. With regard to $V_{Si}^-$, the $^{29}$Si ENDOR measurements on *n*-irradiated 4H-SiC by Wimbauer *et al.*[8] at 9.5 GHz supply evidence that $S=\frac{3}{2}$. However, as shown in this paper the EPR spectrum of $V_{Si}^-$ overlaps with the strong signal of the carbon vacancy and one cannot exclude that the $^{29}$Si ENDOR signals at least partly belong to the carbon vacancy. With regard to $V_{Si}^0$ the observed orientational dependence of the two EPR lines does not prove unambiguously that $S=1$ because the strong signal at $g=2$ of $V_{Si}^-$ may hide the central line of a possible $S=\frac{3}{2}$ spin. In our opinion there is little doubt about the assignment of $S=1$ to $V_{Si}^0$ because the ODMR spectra of Sörman *et al.*,[9] which are characterized by exactly the same *D* values as the EPR spectra, do not show a signal around $g=2$. To support the assignment of $S=\frac{1}{2}$ to $V_C$, $S=1$ to $V_{Si}^0$ and $S=\frac{3}{2}$ to $V_{Si}^-$ we have measured the pulse length needed for the optimum echo signals in our ESE experiments. This pulse length is determined by the matrix element of $S_x$ which describes the transition between the magnetic sublevels for the systems with $S=\frac{1}{2}$, 1, and $\frac{3}{2}$. By expressing $S_x$ in terms of the raising and lowering operators and using the expressions given in Ref. 24 one finds immediately that this matrix element in the case of $S=1$ is a factor $\sqrt{2}$ larger than for $S=\frac{1}{2}$. For $S=\frac{3}{2}$ the matrix elements are a factor $\sqrt{3}$ or 2 larger than for $S=\frac{1}{2}$. We do find these ratios when comparing the pulse lengths needed for the maximum ESE signals of the $V_{Si}^-$ ($S=\frac{3}{2}$), $V_{Si}^0$ ($S=1$), and $V_C$ ($S=\frac{1}{2}$) centers.

Figure 3(b) shows W-band ESE-detected EPR spectra observed at 1.2 K in *n*-irradiated 4H-SiC ($10^{18}$ cm$^{-2}$) for several orientations of the magnetic field with respect to the *c* axis including the magnetic field parallel ($\theta=0°$) and perpendicular ($\theta=90°$) to the *c* axis. The spectra are similar to those in Fig. 3(a) but now they are recorded by ESE detection at low temperature. A very small splitting is present at $B\|c$ similar to that in Fig. 3(a) caused by the difference in the *g* tensors of the quasicubic and hexagonal sites. In particular we could not detect any change in the position of the ESE-detected EPR lines caused by a small but finite zero-field splitting. At 94.9 GHz and 1.2 K we can only observe the $M_S=-\frac{3}{2}\leftrightarrow M_S=-\frac{1}{2}$ transition of this $S=\frac{3}{2}$ spin system because of the large population difference of the sublevels which makes the experiment very sensitive to the presence of a fine-structure splitting. We conclude that the *D* parameter must be $<5\times10^{-5}$ cm$^{-1}$.

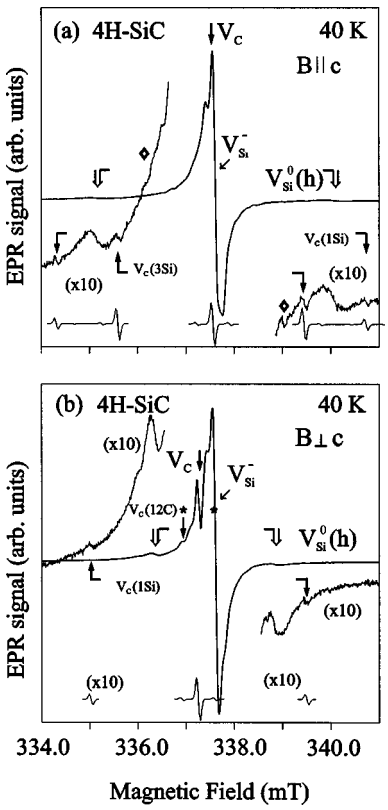


FIG. 4. cw X-band EPR spectra observed at 40 K in *n*-irradiated 4H-SiC (dose of $10^{18}$ cm$^{-2}$) with the magnetic field parallel (a) and perpendicular (b) to the *c* axis. The double vertical arrows indicate the positions of the lines for the $V_{Si}^0$ vacancy ($S=1$) in the *h* site. The oblique solid arrow indicates the position of the central line of the $V_{Si}^-$ vacancy ($S=\frac{3}{2}, D\cong0$). The vertical solid arrows mark the central lines of the carbon vacancy $V_C$. For $B\|c$ the position of this line almost coincides with the position of the central line of the $V_{Si}^0$ vacancy. The vertical solid arrow with an asterisk indicates one of the two lines of the hf interaction with 12 C atoms (12C) in the second shell. The position of the second line is indicated only by an asterisk, because this line is masked by the signal of the $V_{Si}^-$ vacancy. The high-gain spectrum (×10) shows the hf structure for $V_C$ caused by the interaction with one (1Si) and with three (3Si) nonequivalent Si atoms in the first shell for $B\|c$ and the hf interaction with one Si atom in the first shell (1Si) for $B\perp c$. At the bottom of (a) and (b) the simulated spectra are presented. The low-intensity lines labeled by diamonds in the high-gain spectrum of $B\|c$ is caused by the hf interaction with one C in the first shell of the $V_{Si}^-$ vacancy.

Figure 4 shows the cw X-band EPR spectra observed at 40 K in *n*-irradiated 4H-SiC ($10^{18}$ cm$^{-2}$) with the magnetic field parallel (a) and perpendicular (b) to the *c* axis. One can see several groups of signals, two of which were presented already in previous figures. The double vertical arrows indicate the positions of the lines for the $V_{Si}^0$ vacancy ($S=1$) in the *h* site. The oblique solid arrow indicates the position of the central line of the $V_{Si}^-$ vacancy ($S=\frac{3}{2}, D\cong0$). In addition new anisotropic lines, a central line accompanied by hf structure components, are observed. The vertical solid arrows mark these lines which are attributed to $V_C$. For $B\|c$ the position of the central line almost coincides with the

position of the central line of the $V_{Si}^-$ vacancy. The principal values of the $g$ tensor for the central line are $g_\parallel = 2.0032$ and $g_\perp = 2.0048$.

The vertical solid arrow with an asterisk indicates one of two hf lines with a separation from the central line of about 3.4 G. This separation does practically not depend on the orientation. For $B \| c$ this line is almost not observable because of the overlap with the signal of the $V_{Si}^-$ vacancy. The position of the second line is indicated only by an asterisk, because this line is masked by the signal of the $V_{Si}^-$ vacancy. The intensity ratio of the hf component to the central line is about 0.07. This hf component is assumed to arise from the hf interaction with 12 C atoms of the second shell. This is considered as an argument that this spectrum belongs to the isolated carbon vacancy. The simulated spectra for the hf interaction with 12 equivalent C atoms are presented at the bottom of Figs. 4(a) and (b). The value of the hf interaction used for the simulation was 6.4 G.

The high-gain spectrum ($\times 10$) shows the hf structure for $V_C$ due to the interaction with one (1Si) and with three (3Si) nonequivalent Si atoms in the first shell for $B \| c$, and the hf interaction with one Si atom in the first shell (1Si) for $B \perp c$. The high-gain spectrum shows the hf structure with one (64.2-G splitting) and three (38.6-G splitting) nonequivalent Si atoms in the first shell. Further the hf interaction with one Si (44.2-G splitting) in the first shell for $B \perp c$ is observable. The lines caused by hf interaction with the other three Si atoms that are not equivalent are not resolved and are masked by the wings of the $V_{Si}^-$ line and the signals of $V_{Si}^0$. The assignment of the hf lines is marked in the figure. At the bottom the simulated spectra are presented with the intensity of the hf lines multiplied by 10. The intensity of the observed hf signals for the interaction with three Si atoms are less then those simulated because of small misorientations of the crystal which result in a broadening of the hf lines. For $B \perp c$ only the hf interaction with one Si atom was simulated.

The $g$ tensor and hf splitting for the interaction with four Si atoms in the first shell are almost identical to the parameters which were described by Son *et al.*[19] and Bratus' *et al.*[20] for electron-irradiated 4H-SiC crystals and that were attributed by these authors to a carbon-vacancy-related defect. For the isolated carbon vacancy, as it was mentioned, an additional hf structure is observed owing to the interaction with 12 carbon atoms in the second shell. We consider this result as a confirmation to assign this EPR spectrum to the isolated carbon vacancy which we speculate to be in the positive charge state ($V_C^+$). The low intensity lines labeled by diamonds in the high-gain spectrum of $B \| c$ [Fig. 4(a)] are caused by the hf interaction with one C in the first shell of the $V_{Si}^-$ vacancy. The intensities of the EPR spectra $V_{Si}^0$, $V_{Si}^-$, and $V_C$ are comparable and almost proportional to the irradiation dose. Thus we conclude that these three spectra belong to intrinsic defects.

To evaluate the contributions to the fine-structure parameters $D$ for $V_{Si}^0$ and $V_{Si}^-$ we consider the magnetic dipole-dipole interaction between the electron spins and the spin-orbit interaction. There is a simple relation between the contribution of the spin-orbit coupling to the $D$ tensor and the $g$-tensor shift $\Delta g_{ij} = g_{ij} - 2.0023$,[25]

$$D_{ij} = \tfrac{1}{2} \lambda \Delta g_{ij}, \tag{1}$$

where $\lambda$ is the spin-orbit coupling constant. Equation (1) therefore serves to give a rough estimate of the spin-orbit contribution to the observed values of $D$. The spin-orbit coupling in the carbon orbital of $V_{Si}^0$ and $V_{Si}^-$ is taken as $\lambda = 29\ \mathrm{cm}^{-1}$.[26] For the $V_{Si}^0$ vacancy with $S=1$ the $g$ tensor was found to be isotropic, i.e., $|g_\parallel - g_\perp| < 10^{-5}$ and according to (1) $D < 1.45 \times 10^{-4}\ \mathrm{cm}^{-1}$. This value is small compared to the observed zero-field splitting parameter $D$ for the $h$ and $k$ sites in 4H-SiC and 6H-SiC and thus we conclude that in the case of $V_{Si}^0$ the main contribution to $D$ is caused by the dipole-dipole interaction. For the $V_{Si}^-$ it was found that $g_\parallel - g_\perp = 2 \times 10^{-5}$ and according to (1) we predict $D \cong 2.9 \times 10^{-4}\ \mathrm{cm}^{-1}$. Experimentally it was found that $D$ is smaller than the linewidth of about 0.5 G or $0.5 \times 10^{-4}\ \mathrm{cm}^{-1}$. This difference may be partly caused by the reduction of the effective spin-orbit coupling parameter $\lambda$ from its atomic value.

As demonstrated above the two types of vacancies in SiC, $V_{Si}$ and $V_C$, have different properties. The same difference should apply to the behavior of divacancies (or chains of vacancies of various lengths) in SiC. In the carbon-site divacancy the Si-dangling bonds around each carbon vacancy are rather extended and therefore one may expect, like in the case of the divacancy in silicon,[27] that in addition to the anisotropy associated with the vacancy-vacancy direction in the lattice, an additional distortion will be present caused by the Jahn-Teller effect. Watkins and Corbett[27] observed a low-spin ground state with $S = \frac{1}{2}$ for both singly positive and singly negative charge states of the divacancy in silicon. The observations were explained by assuming the presence of a symmetry-lowering Jahn-Teller distortion of the surrounding lattice in order to gain energy via formation of dimerlike bonds between neighboring Si atoms. In contrast, the dangling bonds around the silicon vacancy are strongly localized at the neighboring C atoms and the single negatively charged silicon vacancy[8] shows no symmetry lowering and behaves like the negatively charged vacancy in diamond where a high-spin, orbital singlet state occurs.[17] Similar high-spin configurations (with $S=1$ and $S=\frac{3}{2}$) were observed for divacancies and chains of vacancies of various lengths in diamond.[28] The zero-field splitting parameter $D$ was explained by assuming direct dipole-dipole interaction between distant carbon vacancies. The same situation seems to be present for silicon divacancies in SiC where many triplet states for divacancies were observed[2–4] because high-spin states give rise to the lowest total energies. The silicon-carbon divacancy which was observed in SiC (Refs. 3 and 4) has also a triplet ground state but in this case the situation is not so clear. Thus one should expect that together with a large variety of divacancies with $S=1$ many EPR spectra with $S=\frac{1}{2}$ should be observable that could be connected with carbon divacancies or more complicated carbon-vacancy-related defects. Unfortunately, in this case all the lines are close to $g=2$ and the only hope to separate them is by using high-frequency EPR techniques.

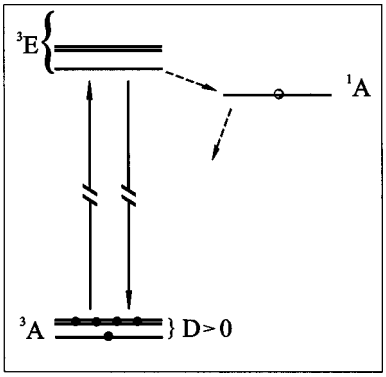


FIG. 5. Suggested energy-level scheme of the $V_{Si}^0$ vacancy in SiC. The double line of the upper sublevels for the $^3A$ and $^3E$ states indicates that these levels are doubly degenerate. For the $^3E$ state only the lower three levels are indicated. The populations of the ground-state energy levels under optical pumping are indicated by different numbers of filled circles. The population of the metastable level $^1A$ is indicated by an open circle to show that its population is much higher than the population of the $^3E$ levels. The radiative and nonradiative transitions are indicated by solid and dashed lines, respectively.

In Fig. 5 a possible energy-level scheme of the $V_{Si}^0$ vacancy in SiC is presented. The $^3A$ ground state, the $^3E$ excited state and the ''metastable'' $^1A$ state are indicated. The double line of the upper sublevels for the $^3A$ and $^3E$ states indicates that these levels are doubly degenerate. Because of the orbital degeneracy the $^3E$ excited state has a complicated structure where spin-orbit, crystal-field, and spin-spin interactions as well as strain in the crystal play a role. For this reason only the lower three levels are indicated. The populations of the energy levels of the ground state under optical pumping are indicated by different numbers of filled circles. The population of the ''metastable'' level $^1A$ is indicated by an open circle to show that its population is higher than the population of the $^3E$ levels. The radiative and nonradiative transitions are indicated by solid and dashed lines, respectively.

The main difference between this scheme and the diagrams considered in earlier papers[4,9,10] lies in the assignments of triplet spin character to the ground- and excited state manifold. The EPR spectrum exhibits spin polarization (non-Boltzmann distribution of the populations)[4] in the illuminated samples, indicating optical pumping among the spin sublevels of the triplet ground state. This observed spin polarization can be explained either by a rotation of the spin axes in the excited triplet state or via intersystem crossing via a metastable singlet state as indicated in Fig. 5. The fact that no Zeeman shift or splitting was observed in the optical experiments of Wagner *et al.*[10] can also be explained with the scheme of Fig. 5. This effect is absent when the Zeeman splitting in the triplet ground state and excited triplet state are similar as is the case if the $g$ factors are close to $g=2.0$ within about 10%. The energy-level scheme presented in Fig. 5 is similar to the scheme for the nitrogen-vacancy ($N$-$V$) defect in diamond.[29,30] Here it was finally established that the ground state is also a triplet state. There have also been extensive discussions about the electronic structure of the ($N$-$V$) defect and its charge state.[31,32] It is now generally believed that the charge state is $(N\text{-}V)^-$ and that there are six valence electrons. From the similarity with the $V_{Si}^0$ vacancy it is clear that the same energy-level scheme can be realized with four valence electrons. Thus it is not excluded that $(N\text{-}V)^+$ with a configuration isoelectronic to $V_{Si}^0$ explains the electronic properties of the ($N$-$V$) defect. Such a four-electron configuration looks more natural and seems to be consistent with all the experimental data.

## IV. CONCLUSION

EPR and ESE studies show that the isolated vacancies $V_{Si}^-$, $V_{Si}^0$ and $V_C$ (most probably the charge state is $V_C^+$) are the dominant intrinsic paramagnetic defects generated by neutron irradiation of SiC to doses up to $10^{19}$ cm$^{-2}$. The high concentrations of these defects, that are almost proportional to the irradiation dose, support the contention that all spectra belong to intrinsic defects. The simultaneous observation of all these defects in high-dose $n$-irradiated SiC crystals shows that the energy-level positions of these defects pin the Fermi level near the middle of the band gap of SiC. This finding is a confirmation of the suggestion that the two charge states of the silicon vacancy that are observed by EPR are separated by one unit of charge.

The W-band EPR spectra observed in complete darkness and at the very low temperature of 1.2 K show that the ground state of $V_{Si}^0$ is a triplet state. The zero-field splitting parameters $D$ are found to be positive. A possible energy-level scheme and optical-pumping process which induces the spin polarization of the ground triplet state of the $V_{Si}^0$ vacancy in SiC is presented. This scheme is similar to that for the well-known ($N$-$V$) defect in diamond. We suggest that the dominant ($N$-$V$) defect in diamond may correspond to a positively charged $(N\text{-}V)^+$ state, iso-electronic to the isolated neutral $V_{Si}^0$ vacancy.

In the EPR spectra of $V_{Si}^-$ in 4H-SiC an anisotropic splitting of the EPR lines is observed. This splitting is assumed to arise from small differences in the $g$ tensor of the quasicubic ($k$) and hexagonal ($h$) sites. The $g$ tensor for the $k$ site $g$ ($k$) is found to be isotropic with $g(k)=2.0032$ and the $g$ tensor of the $h$ site is found to be slightly anisotropic with $g_{\parallel}(h)=g(k)+0.000\,04$ and $g_{\perp}(h)=g(k)+0.000\,02$. Pulsed EPR measurements at 95 GHz confirm that the spin multiplicity of $V_{Si}^-$ is $S=\frac{3}{2}$ in agreement with the results of ENDOR measurements,[8] and that $S=1$ for $V_{Si}^0$. The fine-structure $D$ parameter for $V_{Si}^-$ is close to zero ($D<0.5\times10^{-4}$ cm$^{-1}$).

Anisotropic EPR spectra with $S=\frac{1}{2}$ that are related to carbon vacancies were also observed in $n$-irradiated SiC crystals. The hf interaction with the first shell of Si atoms is almost identical to that observed in electron-irradiated SiC crystals. The additional 6.8-G hf structure with 12 carbon atoms in the second shell that is presented in this paper can be considered as a confirmation for the isolated carbon-vacancy model. The charge state of the carbon vacancy seems to be $V_C^+$, but one cannot exclude the possibility of a negative charge state.

**ACKNOWLEDGMENTS**

This work forms part of the research program of the Technology Foundation STW with financial support from the ''Nederlandse Organisatie voor Wetenschappelijk Onderzoek'' (NWO). P.G.B. acknowledges support by NWO under Grant No. NB 67-286 and by RFBR under Grant No. 00-02-16950.

[1] G. Watkins, in *Deep Centers in Semiconductors*, edited by S. T. Pantelides (Gordon and Breach, New York, 1986), p. 147.
[2] L. A. de S. Balona and J. H. N. Loubser, J. Phys. C **3**, 2344 (1970).
[3] N. M. Pavlov, M. I. Iglitsyn, M. G. Kosaganova, and V. N. Solomatin, Sov. Phys. Semicond. **9**, 845 (1975).
[4] V. S. Vainer and V. A. Il'in, Sov. Phys. Solid State **23**, 2126 (1981).
[5] H. Itoh, M. Yoshikawa, I. Nashiyama, S. Misawa, H. Okumura, and S. Yoshida, IEEE Trans. Nucl. Sci. **37**, 1732 (1990); H. Itoh, A. Kawasuso, T. Ohchima, M. Yoshikawa, I. Nashiyama, S. Tanigawa, S. Misawa, H. Okumura, and S. Yoshida, Phys. Status Solidi A **162**, 173 (1997).
[6] J. Schneider and K. Maier, Physica B **185**, 199 (1993).
[7] M. Kunzer, Ph.D. thesis, Universität Freiburg i.Brsg, 1995.
[8] T. Wimbauer, B. K. Meyer, A. Hofstaetter, A. Scharmann, and H. Overhof, Phys. Rev. B **56**, 7384 (1997).
[9] E. Sörmann, N. T. Son, W. M. Chen, O. Kordina, C. Hallin, and E. Janzén, Phys. Rev. B **61**, 2613 (2000).
[10] Mt. Wagner, B. Magnusson, W. M. Chen, E. Janzén, E. Sörmann, C. Hallin, and J. L. Lindström, Phys. Rev. B **62**, 16 555 (2000).
[11] H. J. Von Bardeleben, J. L. Cantin, G. Battistig, and I. Vickridge, Phys. Rev. B **62**, 10 126 (2000).
[12] H. J. von Bardeleben, J. L. Cantin, L. Henry, and M. F. Barthe, Phys. Rev. B **62**, 10 841 (2000).
[13] Mt. Wagner, N. Q. Thinh, N. T. Son, P. G. Baranov, E. N. Mokhov, C. Hallin, W. M. Chen, and E. Janzén, *Proceedings of the International Conference on Silicon Carbide and Related Materials 2001, Tsukuba, Japan* [Mater. Sci. Forum **389–393,** 501 (2002)].
[14] F. P. Larkin and A. M. Stoneham, J. Phys. C **3**, L112 (1970).
[15] P. Deak, J. Miro, A. Gali, L. Udvardi, and H. Overhof, Appl. Phys. Lett. **75**, 2103 (1999).
[16] L. Torpo, R. M. Nieminen, K. E. Laasonen, and S. Poykko, Appl. Phys. Lett. **74**, 221 (1999).
[17] A. Zywietz, J. Furthmuller, and F. Bechstedt, Phys. Rev. B **59**, 15 166 (1999).
[18] P. G. Baranov, E. N. Mokhov, S. B. Orlinskii, and J. Schmidt, *Proceedings of the 21st International Conference on Defects in Semiconductors 2001, Giessen, Germany* [Physica B **308–310,** 680 (2001)].
[19] N. T. Son, P. H. Hai, and E. Janzén, Mater. Sci. Forum **353–356**, 499 (2001).
[20] V. Ya. Bratus', I. N. Makeeva, S. M. Okulov, T. L. Petrenko, T. T. Petrenko, and H. J. von Bardeleben, Mater. Sci. Forum **353–356**, 517 (2001).
[21] J. A. J. M. Disselhorst, H. J. van der Meer, O. G. Poluektov, and J. Schmidt, J. Magn. Reson., **115**, 183 (1995).
[22] V. G. Grachev, Zh. Eksp. Teor. Phys. **92**, 1834 (1987) [Sov. Phys. JETP **65**, 1029 (1987)].
[23] Th. Lingner, S. Greulich-Weber, J.-M. Spaeth, U. Gerstmann, E. Rauls, Z. Hajnal, Th. Frauenheim, and H. Overhof, Phys. Rev. B **64**, 245212 (2001).
[24] C. P. Slichter, *Principles of Magnetic Resonance*, Springer Series in Solid-State Sciences, Vol. 1 (Springer-Verlag, Berlin, 1978), p. 15.
[25] G. D. Watkins, Phys. Rev. **155**, 802 (1967).
[26] N. M. Atherton, *Principles of Electron Spin Resonance* (Ellis Horwood PTR, Prentice-Hall, Englewood Cliffs, NJ, 1993), p. 42.
[27] G. D. Watkins and J. M. Corbett, Phys. Rev. **138**, A543 (1965).
[28] J. H. N. Loubser and J. A. van Wyk, Rep. Prog. Phys. **41**, 1201 (1978).
[29] D. A. Redman, S. Brown, R. H. Sands, and S. C. Rand, Phys. Rev. Lett. **67**, 3420 (1991).
[30] A. Dräbenstedt, L. Fleury, C. Tietz, F. Jelezko, S. Kilin, A. Nizovtzev, and J. Wrachtrup, Phys. Rev. B **60**, 11 503 (1999).
[31] J. P. Goss, R. Jones, P. R. Briddon, G. Davies, A. T. Collins, A. Mainwood, J. A. van Wyk, J. M. Baker, M. E. Newton, A. M. Stoneham, and S. C. Lawson, Phys. Rev. B **56**, 16 031 (1997), and references therein.
[32] A. Lenef and S. C. Rand, Phys. Rev. B **56**, 16 033 (1997).